Supporting Information

Ding et al. 10.1073/pnas.1302844110

SI Text

Empirical Granular Force Laws in the Resistive Force Theory

To obtain the empirical force laws for the forces acting on the sandfish, we dragged a stainless-steel cylinder (radius $r = 1.58$ cm and length $l = 4$ cm) in 0.3-mm glass beads at a constant velocity (10 cm/s) and measured the resulting perpendicular and parallel forces for angles ψ between the element and its displacement direction. The perpendicular $F_{\perp}$ and parallel $F_{||}$ components of the force on the cylindrical surface of the rod as a function of ψ are approximated as

$$\begin{aligned} F_{\perp} &= 2lr(C_s \sin\beta_0 + C_F \sin\psi), \\ F_{||} &= 2lrC_F \cos\psi, \end{aligned} \qquad \text{[S1]}$$

where $\tan\beta_0 = \cot\gamma_0 \sin\psi$, $C_S = 0.51\text{N/m}^2 \times 10^{-4}$, $C_S = 0.28\text{N/m}^2 \times 10^{-4}$, and $\gamma_0 = 13.84°$. Details of the empirical force laws are provided in Maladen et al. (1).

Small-Amplitude Swimming in a Viscous Fluid

For the small (infinitesimal) amplitude, A, case, $\dot{x}_{\text{CoM}} \to 0$ because previous studies (e.g., ref. 2) showed $\dot{x}_{\text{CoM}} \propto A^2$ for swimming in a viscous fluid. Due to the symmetry of a sinusoidal wave in the lateral direction, $F_{\text{net},y} = 0$ and $\dot{y}_{\text{CoM}} = 0$. The contribution to forward motion from small rotations is negligible; therefore, the lateral position and velocity of the body in the laboratory frame can be simplified as

$$\begin{aligned} y(x,t) &= (x-\pi)\theta + A\sin(x+t) \\ v_y(x,t) &= \dot{y}(x,t) = A\cos(x+t) + \dot{\theta}(t)(x-\pi). \end{aligned} \qquad \text{[S2]}$$

Using viscous resistive forces, the torque balance equation in Eq. **2** becomes

$$\begin{aligned} &\tau_{\text{net}}(t) = 0 \\ &\int_0^{2\pi} -\dot{y}(x,t)(x - x_{\text{CoM}})\, dx = 0 \\ &\theta(t) = \frac{3}{\pi^2} A\cos t \\ &\Rightarrow y(x,t) = A\sin(x+t) + \frac{3}{\pi^2} A\cos t(x-\pi). \end{aligned} \qquad \text{[S3]}$$

Elastic and Damping Properties of the Sandfish Body

Experiment 1: Dynamic Bending Tests. Torque vs. angle work loops occurred in a clockwise direction for all sandfish ($n = 3$) (Fig. 7 and Table S1), indicating energy dissipation. Elasticity changed between the animals tested and increased with speed (Table S2) within a range of $1 - 20°$/s. Average elasticity across all animals at 1°/s was 0.12 N·cm/rad; at 10°/s, it was 0.17 N·cm/rad; and at 20°/s, it was 0.18 N·cm/rad. We found torque at zero displacement was constant between 1, 10, and 20°/s ($P > 0.05$), leading to a decreasing damping coefficient, c, with increasing speed. For the hysteretic damping model, we found that the structural damping coefficient, h, was independent of angular speed between 1 and 20°/s ($P > 0.05$), resulting in a decreasing loss factor, η ($P < 0.0001$), due to the increasing body stiffness, K. Trends for estimated torque during swimming using calculated K and c are shown in Fig. S4. Torque from hysteretic damping is proportional to torque from viscous damping and follows the same trends.

For the experiment in which a sandfish was rotated at 1, 10, 20, 50, and 100°/s (the maximum achievable value with our system) (Fig. S4, *Inset*), we found similar results for rotation rates below 20°/s. The stiffness coefficient and the associated torque increased from 1 to 20°/s, whereas the torque from both viscous and hysteretic damping remained approximately constant. In accord with this, the area enclosed by the hysteresis loop (E_{loss}) was also constant. However, from 20 to 100°/s, the stiffness coefficient and elastic torque remained constant, whereas both damping torques increased, indicating that viscous damping may be a better model of the system at high angular velocities. The average torque at 240°/s (the average angular velocity of segments during sand-swimming) was calculated using the average stiffness and viscous damping coefficient at (20 °/s). We estimated that torque due to bending stiffness is 0.09 ± 0.03 N·cm, which is ~2.3% of the torque exerted on the sandfish by the external media. The torque due to viscous damping is 0.06 ± 0.034 N·cm, and it is 1.5% of total external force. By interpolating the hysteretic damping torque vs. angular speed curve after 20°/s, we estimated similar torque (0.06 N·cm) at 240°/s compared with the viscous model.

Experiment 2: Pendulum Swing Tests. Fitting a viscoelastic model and hysteretic model (Fig. S6) yielded small spring coefficients ($K = 0.006 \pm 0.1$) with some calculated values in the negative range (Table S3). We explain this because the torque due to gravity is large compared with the torque from passive elasticity during bending (on average, 7% of the gravitational force), and therefore is not beyond the error of approximation. However, this finding confirms that passive elasticity in sandfish is small.

The viscous damping coefficient (0.012 ± 0.006 N·cm·s·rad^{-1}) was on the same order as that measured in the bending test at 20°/s (Table S3). The loss factor also followed the pattern predicted by the bending test. The value of η was ~0.38 ± 0.22 N·cm·rad^{-1}. Therefore, the average torque due to hysteretic damping is 0.009 ± 0.004 N·cm (less than 0.3% of the torque due to the external load). Regardless of the model chosen, viscous or hysteretic, torque due to passive damping was small.

In conclusion, both the swinging test and the bending test show that passive stiffness and damping are small compared with the force due to the external load (<5% combined) and confirm the assumptions used in our model.

Estimation of the Torque from Inertial Force for the Sand-Swimming of the Sandfish

The maximal inertial force per unit length can be estimated from the product of the maximal acceleration and body mass per unit length: $F_{\text{inertial}} = (2\pi f)^2 A \times m/L \approx (6.28 \times 2\text{Hz})^2 \times 1.7\text{ cm} \times 17.3\text{ g}/14.7\text{ cm} = 0.003$ N/cm. We estimate that the effective density of the glass beads is $\rho_{\text{eff}} = \rho_{\text{glass}}\phi = 1.5\text{ g/cm}^3$ and the volume of material that moves with the body is about the same as that of the body itself. Then, the total inertial force is about 0.008 N/cm. Assuming the ratio between the torque from inertial force and resistive force is the same as the ratio between the forces $\left(\frac{0.008\text{ N/cm}}{0.8\text{ N/cm}} = 0.01\right)$, we estimate the torque from inertial force as 4 N·cm × 0.01 = 0.04 N·cm.

1. Maladen RD, Ding Y, Li C, Goldman DI (2009) Undulatory swimming in sand: Subsurface locomotion of the sandfish lizard. *Science* 325(5938):314–318.

2. Gray J, Hancock G (1955) The propulsion of sea-urchin spermatozoa. *J Exp Biol* 32: 802–814.

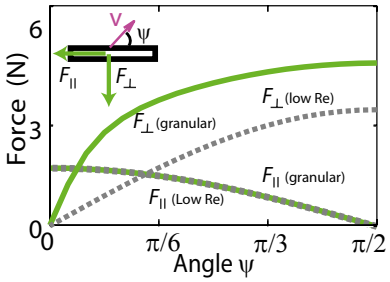

Fig. S1. Empirical force relationships used in the resistive force theory model [adapted from the study by Maladen et al. (1)]. Green solid lines represent the perpendicular ($F_{\perp}$) and parallel ($F_{||}$) components of the force. Dashed gray lines correspond to $F_{\perp}$ and $F_{||}$ calculated for an infinitely long slender ellipsoid in a low Reynolds number fluid by choosing a velocity that fits $F_{||}$ vs. ψ.

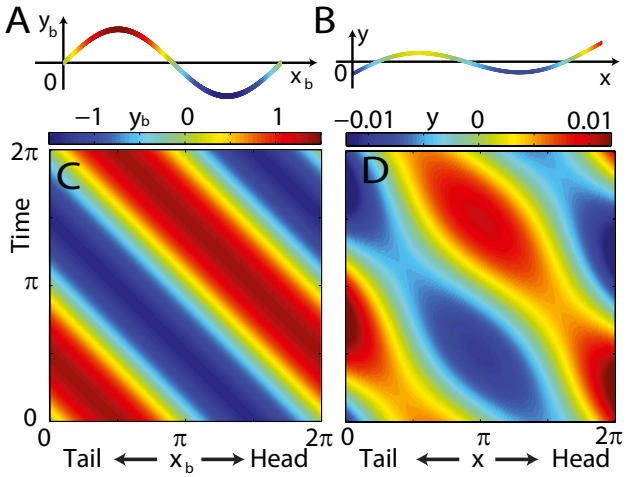

Fig. S2. Lateral position of the swimmer in its body frame (*A*) and in the laboratory frame (*B*). (*A* and *C*) Position of the model swimmer in the body frame is a traveling sinusoidal wave with $A/\lambda = 0.22$. Color represents lateral displacement y_b. (*B* and *D*) Position of a swimmer in a viscous fluid in the laboratory frame. The swimmer uses a sinusoidal wave with a small amplitude ($A/\lambda = 0.01$ in this example) and the fore-aft distance is kept as 2π. Color represents lateral displacement y. The analytical expression is provided in Eq. **S3**.

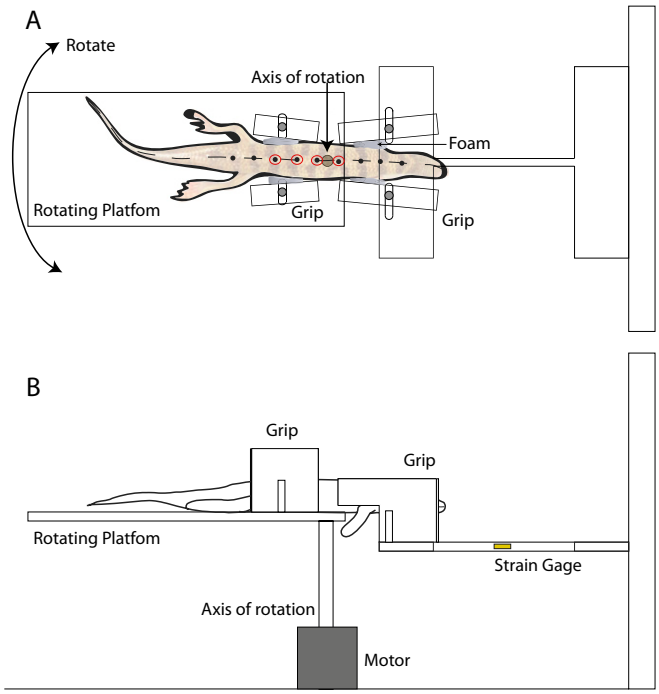

Fig. S3. The body elasticity is experimentally measured by bending the sandfish body and measuring the resulting torque. (*A*) Top and (*B*) side views of the experimental setup are shown. Adjustable grips hold the animal at different snout-to-vent length (SVL) locations (0.5 and 0.6 SVL) and are attached to a rigid platform and to a rotating platform, respectively. A motor rotates the anterior region of the sandfish through $\pm 15°$, and resulting bending moment is measured with strain gauges. Black circles were marked on the animal's midline at increments of 0.1 SVL. The best-fit line through the markers circled in red was used to calculate angle θ.

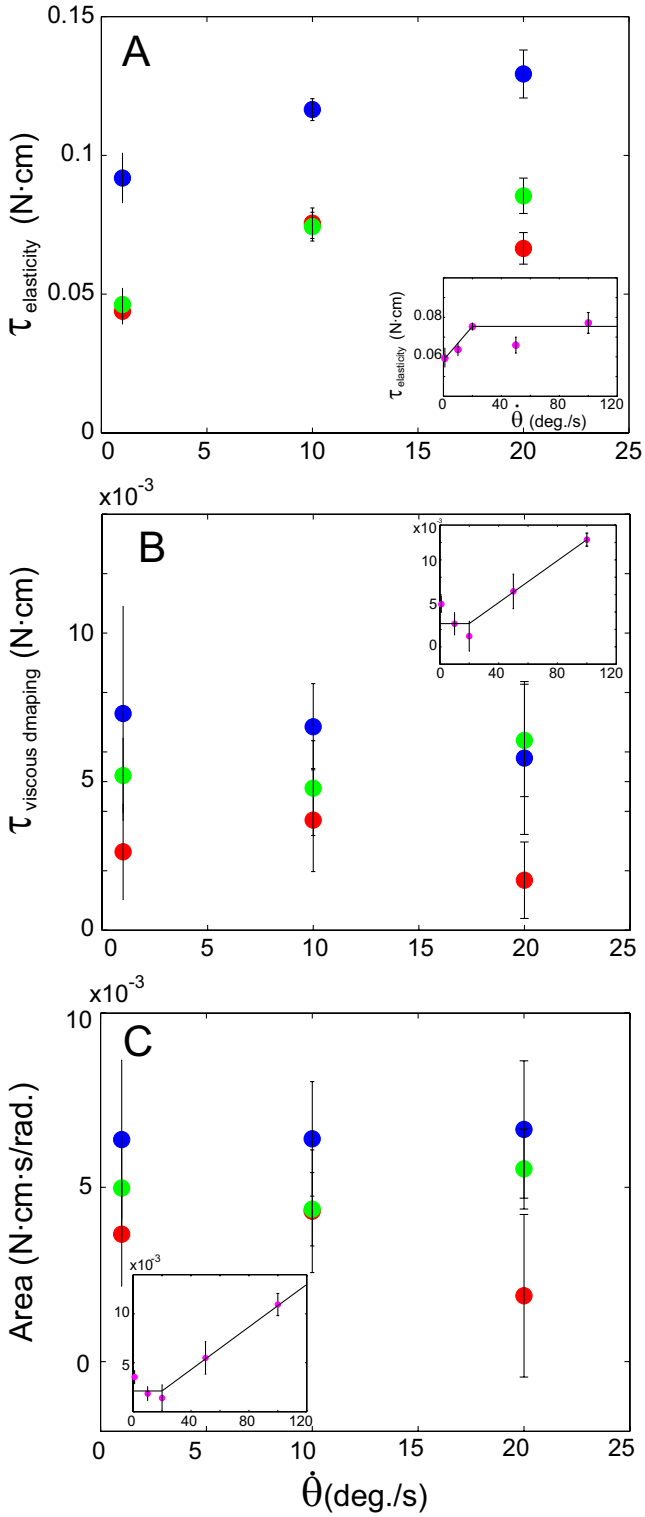

Fig. S4. Estimated average torque using calculated elasticity and damping coefficients shown for animal 1 (blue circles), animal 2 (red circles), and animal 3 (green circles) ($n = 8$ trials each). (*Insets*) Trends for the experiment at higher speeds (magenta circles). (*A*) Torque slightly increases due to a higher K up to 20°/s and then plateaus afterward. (*B*) Torque due to viscous damping remains constant (due to deceasing c) up until 20° and increases afterward (due to constant c). (*C*) Area contained within the best-fit curves between the torque and angle is independent of speed before 20°.

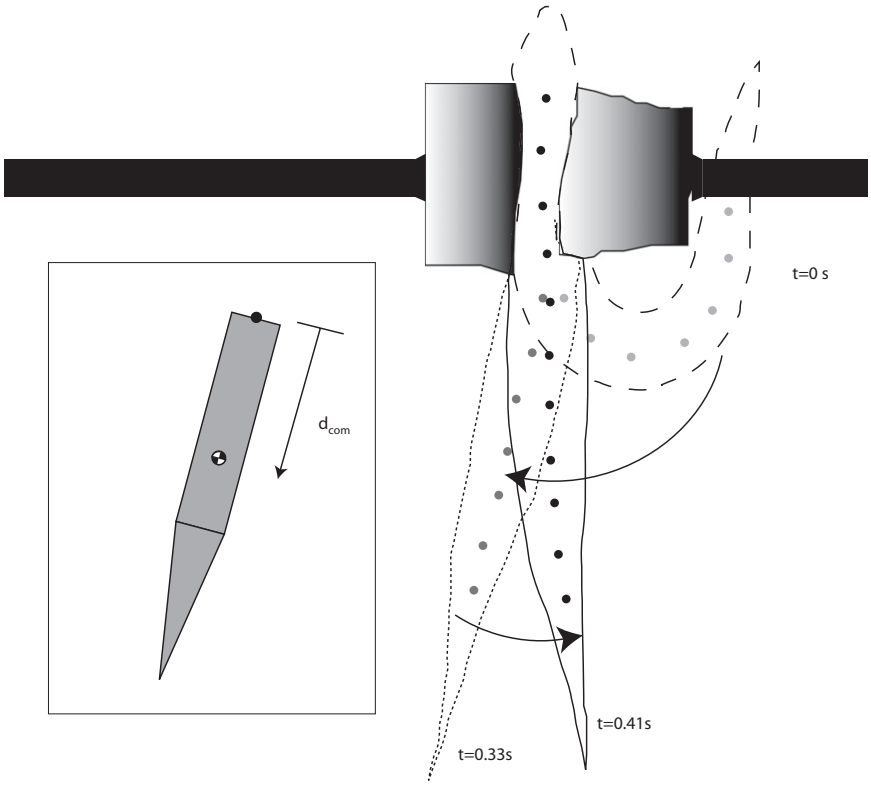

Fig. S5. Swing test to measure passive body properties at natural frequencies. Sandfish were clamped with soft foam to restrict movement anterior to 0.5 SVL. The initial position is shown (dashed outline, $t = 0$ s). The angle is calculated after the first half-cycle (dotted outline, $t = 0.33$ s) when the angle relative to 0.5 SVL and bending is smaller. (*Inset*) Sandfish body is modeled as a cylinder and a cone with uniform density, where d_{com} is the distance to the center of mass.

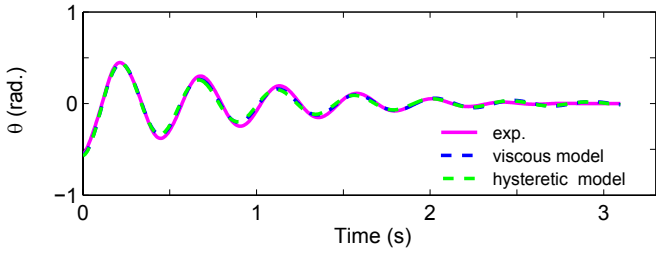

Fig. S6. Representative angle vs. time trajectory for animal 1 during a pendulum swing test. The pink line represents the experiment, the blue dashed line is the viscous model, and the green dashed line is the hysteretic model with best-fit parameters.

Table S1. Mass and size of three sandfish used to estimate passive body properties

Sandfish	Mass, g	Snout-to-vent length, cm	Body length, cm	Width, cm	Height, cm
1	25	10.1	15.7	1.6	1.2
2	16	8.6	14.5	1.5	1.1
3	15	8.2	13.4	1.5	1.1

Sandfish 2 was used again for the high-speed rotation test.

Table S2. Work loop parameters

	Statistics					Mean ± SD	
Variable	Source	df	*F*	*P*	Animal no.	1°/s	10°/s	20°/s
K, N·cm/rad	Frequency	1	151.7	<0.0001	Sandfish 1	0.175 ± 0.017	0.222 ± 0.008	0.247 ± 0.017
	Animal	2	214.62	<0.0001	Sandfish 2	0.084 ± 0.009	0.144 ± 0.011	0.127 ± 0.011
	Frequency × animal	2	4.14	0.0203	Sandfish 3	0.088 ± 0.011	0.142 ± 0.010	0.163 ± 0.012
	Error	66			Overall	0.116 ± 0.045	0.170 ± 0.040	0.179 ± 0.053
c, N·cm·s·rad^{-1}	Frequency	1	82.36	<0.0001	Sandfish 1	0.418 ± 0.207	0.039 ± 0.008	0.017 ± 0.007
	Animal	2	5.48	0.0063	Sandfish 2	0.151 ± 0.092	0.021 ± 0.010	0.005 ± 0.004
	Frequency × animal	2	5.85	0.0046	Sandfish 3	0.298 ± 0.072	0.027 ± 0.009	0.018 ± 0.005
	Error	66			Overall	0.289 ± 0.172	0.029 ± 0.012	0.013 ± 0.008
η	Frequency	1	21.01	<0.0001	Sandfish 1	0.157 ± 0.0718	0.117 ± 0.023	0.089 ± 0.037
	Animal	2	12.65	<0.0001	Sandfish 2	0.123 ± 0.073	0.098 ± 0.044	0.050 ± 0.037
	Frequency × animal	2	0.04	0.9593	Sandfish 3	0.231 ± 0.078	0.128 ± 0.044	0.150 ± 0.04
	Error	66			Overall	0.170 ± 0.085	0.115 ± 0.039	0.096 ± 0.057
E_{loss}, N·cm·rad^{-1}	Frequency	1	0.39	0.5355	Sandfish 1	0.006 ± 0.002	0.006 ± 0.002	0.007 ± 0.002
	Animal	2	19.7	<0.0001	Sandfish 2	0.004 ± 0.001	0.004 ± 0.002	0.002 ± 0.002
	Frequency × animal	2	2.22	0.1168	Sandfish 3	0.005 ± 0.001	0.004 ± 0.001	0.006 ± 0.001
	Error	66			Overall	0.005 ± 0.002	0.005 ± 0.002	0.005 ± 0.003

One-way analysis of covariance table testing effect of oscillation frequency and animal on stiffness, *K;* viscous damping, *c*; loss factor, η; and area, E_{loss}. Average values are shown and separated by speed and animal.

Table S3. Average swing test parameter values (mean ± SD) using viscous and hysteretic damping models for each sandfish and for all data (overall)

	Viscous damping model			Hysteretic damping model		
Animal no.	Osc. freq., s^{-1}	*K*, N·cm·rad^{-1}	*c*, N·cm·s·rad^{-1}	Osc. freq., s^{-1}	K_v, N·cm·rad^{-1}	η
Sandfish 1	2.21 ± 0.04	−0.115 ± 0.030	0.009 ± 0.002	2.20 ± 0.05	−0.127 ± 0.016	0.183 ± 0.015
Sandfish 2	2.70 ± 0.08	0.092 ± 0.035	0.020 ± 0.005	2.54 ± 0.02	−0.016 ± 0.007	0.698 ± 0.103
Sandfish 3	2.73 ± 0.01	0.055 ± 0.037	0.009 ± 0.001	2.69 ± 0.08	0.039 ± 0.029	0.320 ± 0.025
Overall	2.54 ± 0.26	0.006 ± 0.100	0.012 ± 0.006	2.47 ± 0.23	−0.036 ± 0.075	0.383 ± 0.224

Osc. freq., oscillation frequency.

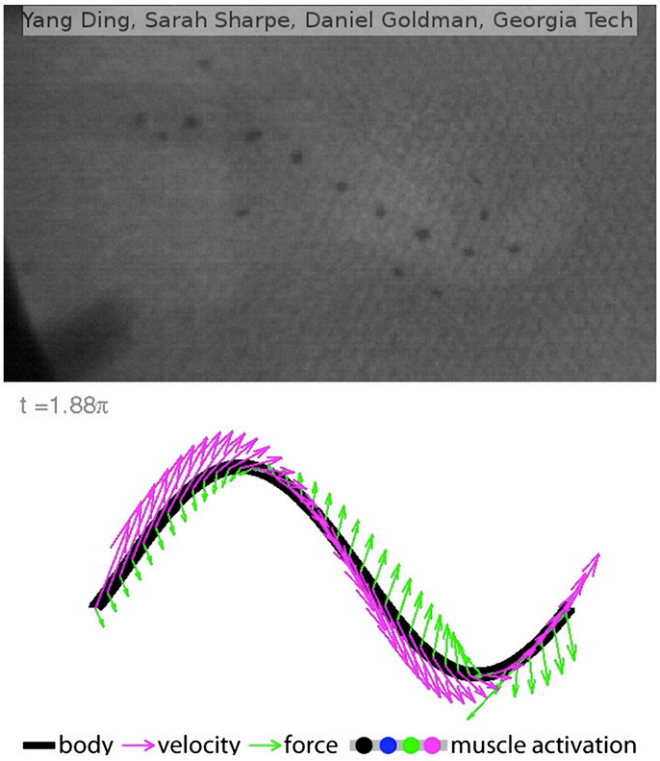

Movie S1. Muscle activation of a sandfish during sand-swimming from the electromyogram experiment (upper half) and the resistance force theory model (lower half). Subsurface swimming of the sandfish is recorded using high-speed X-ray imaging. Black opaque markers (black circles) are attached to the exterior midline to facilitate tracking. Colored dots indicate muscle activation at 0.5, 0.7, 0.9, and 1.1 SVLs, respectively. The thick gray line also indicates muscle activation in the model. Green arrows represent forces. Magenta arrows represent velocities. The experiment in this movie is slowed by 12.5×.

Movie S1